Nuclear Materials and Energy 12 (2017) 1219–1223

Contents lists available at ScienceDirect

Nuclear Materials and Energy

journal homepage: www.elsevier.com/locate/nme

Wide-range evaluation of the deposition layer thickness distribution on the first wall by reflection coefficient measurements

G. Motojima[a,b,*], N. Yoshida[c], S. Masuzaki[a], R. Sakamoto[a,b], M. Tokitani[a,b], H. Tanaka[a,b], T. Murase[a], D. Nagata[a], K. Matsumoto[d], M. Miyamoto[e], M. Yajima[a], M. Sakamoto[f], H. Yamada[a,b], T. Morisaki[a,b], the LHD Experiment Group[a]

[a] National Institute for Fusion Science, National Institutes of Natural Sciences, 322-6 Oroshi-cho, Toki, Gifu 509-5292, Japan
[b] SOKENDAI (The Graduate University for Advanced Studies), 322-6 Oroshi-cho, Toki, Gifu 509-5292, Japan
[c] Research Institute for Applied Mechanics, Kyushu University, 6-1, Kasuga, Fukuoka 812-8580, Japan
[d] Honda R & D Co. Ltd., 4630 Shimotakanezawa, Haga-machi, Tochigi 321-3393, Japan
[e] Department of Material Science, Shimane University, Matsue, Shimane 690-8504, Japan
[f] Plasma Research Center, University of Tsukuba, 1-1-1 Tennodai, Tsukuba, Ibaraki 305-8577, Japan

ARTICLE INFO

Article history:
Received 13 July 2016
Revised 3 March 2017
Accepted 29 April 2017
Available online 12 May 2017

Keywords:
Reflection coefficient
Color analyzer
Deposition layer
Wall retention
Helium

ABSTRACT

A simple method to evaluate the thickness distribution of the deposition layer formed on the first wall is proposed using an innovative measurement concept of the optical reflection coefficient, which is measured as the RGB (red, green, blue) value using a compact color analyzer. Analysis of the samples exposed to plasmas during an experimental campaign shows the relationship between the thickness of the deposition layer and the reflection coefficient, which is followed by the single layer model. The reflection coefficient clearly indicates the thickness of the deposition layer between 10 and 100 nm. The reflection coefficients of stainless steel plates on the helically twisted coil in one of the 10 toroidal sections of the vacuum vessel in the Large Helical Device (LHD) are measured. There is almost no deposition layer on the inner side of the torus, however, the deposition layer reaches a thickness of over 100 nm on the first wall near the divertor region. On the outer side of the torus, almost the entire area is covered by the deposition layer. Reflection coefficient measurements indicate that approximately 60% of the area on the measured coil can is coated with a deposition layer over 10 nm thick, which suggests that this area plays a role in the wall retention.

1. Introduction

Fuel retention in the wall is an important issue for the control of the plasma density in fusion devices. In the Large Helical Device (LHD), analysis of the global particle balance is conducted in a long-pulse 48 min helium discharge heated by ion cyclotron resonance heating (ICH) + electron cyclotron heating (ECH) ($1.2\,\mathrm{MW} \times 48\,\mathrm{min} = 3.4 \times 10^3\,\mathrm{MJ}$) [1]. Experimental observations show that the wall retention of helium has phased characteristics and the differences in the plasma facing materials, which are the stainless steel first wall and the graphite divertor, could explain the wall retention [2]. In this discharge, 60% of helium particles are absorbed in the wall. A co-deposition layer mainly composed of carbon is formed on the plasma facing components, and specimen analysis shows that the retention amount is proportional to the thickness of the deposition layer for thickness of 40 nm or less [3]. Thus, the deposition layer is possibly a contributing factor to the wall retention in the LHD.

The key issue for verifying the contribution of the deposition layer to the helium retention in the LHD is a quantitative evaluation of the deposition layer over the entire area of the vacuum vessel. Specimen analysis is commonly employed to evaluate the thickness and microscopic structure of a deposition layer. However, this is difficult to achieve for the entire area of a large fusion device with only finite specimens. In addition, the analysis of each specimen is time consuming. Thus, analysis of the color equivalent to the reflection coefficient, which is dependent on the thickness of the deposition layer, was conducted as a new technique in TEXTOR-94 [4] and ASDEX-U [5]. In these devices, the hue of color tone was measured in order to derive the thickness of the

* Corresponding author at: National Institute for Fusion Science, National Institutes of Natural Sciences, 322-6 Oroshi-cho, Toki, Gifu 509-5292, Japan
E-mail address: motojima.gen@lhd.nifs.ac.jp (G. Motojima).

http://dx.doi.org/10.1016/j.nme.2017.04.018

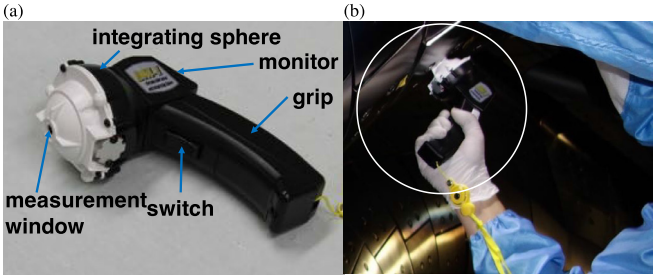

Fig. 1. (a) Photograph of the color analyzer and (b) photograph of the experimental set up of the color analyzer surrounded in a circle.

Table 1
Specifications of the color analyzer.

Measurement	RGB (Red, Green, Blue) HSV (Hue, Saturation, Value)
Measurement window diameter	Φ8.1 mm
Internal diameter of integrating sphere	Φ47 mm
Light source	White LED
RGB range	0~1023
Weight	~160 g
Measurement time	3 s
Record	USB memory installed in analyzer

deposition layer. A CCD color camera was used on the areas of test samples in TEXTOR, and a photograph camera was used on the divertor tiles in ASDEX-U. As a result, the deposition layer thickness was successfully estimated. However, the measurement area was limited and did not extend to the wide area covering the vacuum vessel. Here, we present an innovative concept using reflection coefficient measurements that provides a wide-range evaluation of the deposition layer distribution.

The outline of this paper is as follows. In Section 2, the compact color analyzer used in this study is described. The experimental results, which show the relation between the reflection coefficient and the thickness of the deposition layer and the wide-range evaluation of the thickness distribution, are described in Section 3. A discussion and summary are provided in Section 4.

2. Experimental set up: a compact color analyzer for RGB measurement

A compact color analyzer developed by the Hitachi Kinzoku Corporation was utilized for *in situ* optical reflection measurements [6]. A photograph of the color analyzer is shown in Fig. 1(a). The analyzer has an LED integrating sphere. The incident light from the integrating sphere is spread as homogeneous light by a diffuser and is directed onto an object. A photodiode sensor captures the light reflected from the object and outputs the wavelength integrated intensity of the emission from each of three specific visible wavelength ranges, which have peaks at 615 nm (red), 540 nm (green), and 465 nm (blue). The analyzer can measure each of the RGB (red, green, blue) wavelength regions but also the hue, saturation, and brightness (HSV). However, the RGB values are the focus of this study. The specification of the color analyzer is summarized in Table 1. The color analyzer is user-oriented and easy to carry into the vacuum vessel during a maintenance break for measuring the reflection of plasma facing materials as shown in Fig. 1(b). The color analyzer is calibrated using a color guide to ensure accuracy of the intensities [7]. The calibration results are summarized as follows. Firstly, there are some offset values in each of the RGB values. Secondly, there is the same tendency of the offset for each of the RGB values. Thirdly, the intensity sensitivity is higher for the high RGB values than for the low RGB values. The data are fitted and the RGB values are calibrated from a polynomial fitting curve.

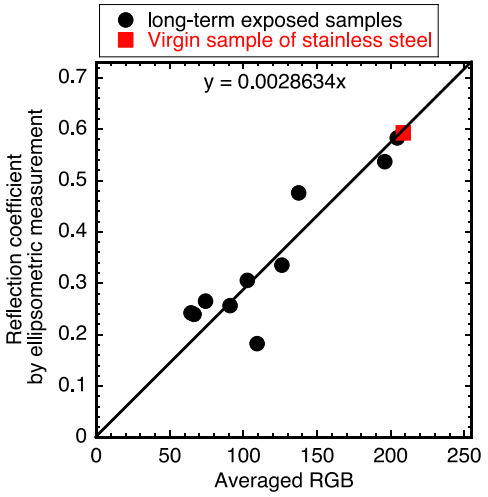

Fig. 2. Relationship between the reflection coefficient by the ellipsometric measurement and the averaged RGB measured by the color analyzer. Circles show the long-term exposed samples and the square shows the virgin sample of stainless steel.

3. Experimental results

3.1. Relation between the reflection coefficient and RGB

To investigate the consistency of the reflection coefficient with the RGB value, the reflection coefficient of long-term exposed samples was evaluated by ellipsometric measurement at Shimane University [8]. The stainless steel samples were placed at various positions on the first wall in one toroidal section of the LHD during the 2014 plasma experiment campaign (18th plasma experiment campaign). The RGB values of the samples were simultaneously measured with the color analyzer. Fig. 2 shows the reflection coefficient as a function of the averaged RGB, which is the average of the three R, G, and B values. The reflection coefficient of the virgin sample of the stainless steel is also plotted in the figure. A linear relation is observed between the reflection coefficient and the RGB value at the samples, which indicates that the RGB value corresponds to the reflection coefficient. The surface roughness may affect the reflection coefficient measurement. However, the effect of surface roughness on the visible wavelength is not significant because the roughness measured by TEM observation was less than 100 nm, which is sufficiently lower than the visible light wavelength.

3.2. Evaluation of deposition layer thickness by TEM observation

To estimate the thickness of the deposition layer from the reflection coefficient data, the relation between them must be clarified. The thickness of the deposition layer can be evaluated from these long-term exposed samples using a focused ion beam system and transmission electron microscopy (TEM). Fig. 3 shows cross-sectional TEM images of the samples. In some samples, the boundary of the deposition layer was difficult to identify. At the same time, the protection of the surface of the samples is necessary to prevent the damage of the sample surface during focused ion beam fabrication. Therefore, tungsten was deposited on the surface. Various thicknesses of the deposition layer in the range between 2 and 1400 nm were observed. The cross-sectional TEM images of the samples show interesting characteristics of the structures in the deposition layer and the base plate where blistering

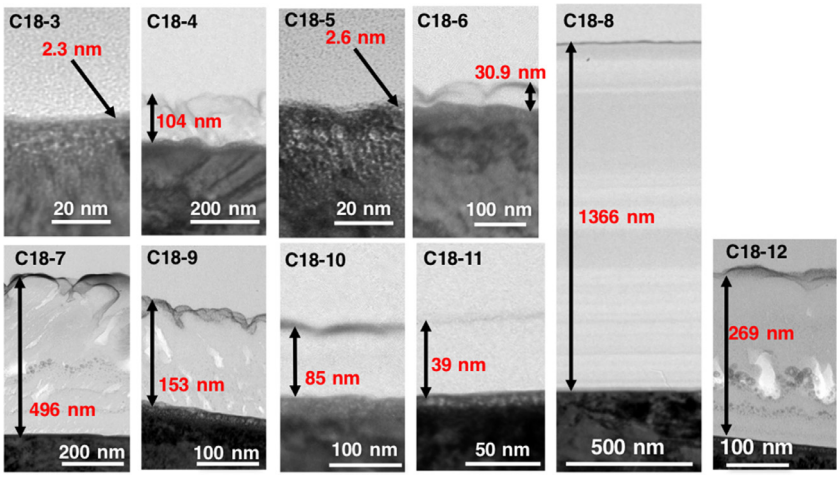

Fig. 3. Cross-sectional TEM images of the long-term exposed samples. Various thicknesses of the deposition layer are observed. Tungsten is deposited on the surface in order to clarify the boundary.

has occurred. However, here we focus on the evaluation of the deposition layer thickness. Therefore, the characteristics of the structures will be reported elsewhere.

3.3. Compatibility of a single layer model with experimental result

To discuss the relationship between the deposition layer thickness and the reflection coefficient, a single layer model was employed. With a simple three-phase model (atmosphere, deposition layer, and substrate area), the reflection coefficient of light, R, can be expressed as follows [9]:

$$\phi = \frac{2\pi N_f d \cos\theta}{\lambda}, \tag{1}$$

$$r = \frac{r_0 + r_1 \exp(i2\phi)}{1 + r_1 r_0 \exp(i2\phi)}, \tag{2}$$

$$R = |r|^2 \tag{3}$$

where ϕ, λ, and θ represent the phase factor, the wavelength, and the incident angle of the light, respectively. N_f and d are the refractive index and the deposition layer thickness, respectively. r represents the overall electric field of the light, while r_0 and r_1 are the Fresnel reflection coefficients at the atmosphere-layer boundary and the layer-substrate boundary, respectively. This simple model shows that the reflection coefficient is dependent on the deposition layer thickness. Here, the ratio of s-polarized light and p-polarized light is assumed to be 1:1. In addition, a complex index of refraction for the deposition layer is used at $n = 1.24$ and $k = 0.98$ approximated by least square approximation, which is similar to the ellipsometric measurement at R ($\lambda = 615$ nm), G ($\lambda = 540$ nm), and B ($\lambda = 465$ nm). Furthermore, the complex index of refraction for a mother sample was evaluated at $n = 1.5$ and $k = 2.9$. The thickness of the deposition layer as a function of the reflection coefficient using the single layer model is shown in Fig. 4. The thickness between 10 and 100 nm shows the clear dependence on the reflection coefficient. The tendency of the single layer model was the same as that for the reflection measurements with the color analyzer and ellipsometric measurements. Therefore, in this study, the relationship between the reflection coefficient and the thickness of the deposition layer indicates that the single layer model is valid.

3.4. Distribution of the reflection coefficients on the coil

The toroidal section where the reflection coefficients were measured with the color analyzer is the same as that of the mounted

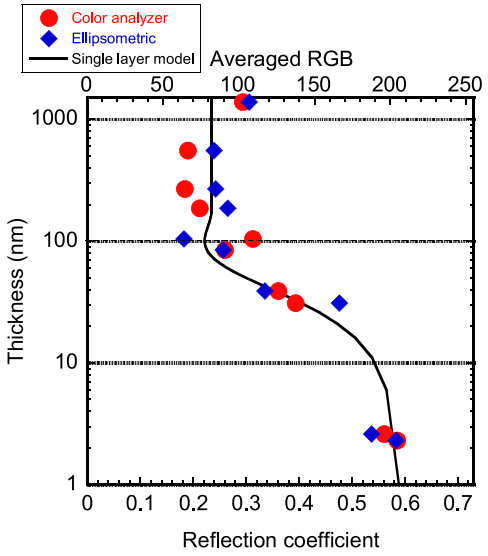

Fig. 4. Thickness of the deposition layer as a function of the reflection coefficient and averaged RGB. Circles and diamonds represent the results of the color analyzer and of the ellipsometric measurements, respectively. Solid line shows the result from the single layer model. In the model, the refractive index is set at $n = 1.24$ and $k = 0.98$ in the deposition layer and at $n = 1.5$ and $k = 2.9$ in the mother sample.

long-term samples. The RGB values were measured for the stainless steel plates on the helically twisted coil in one of the 10 toroidal sections of the vacuum vessel in the LHD. The number of measured stainless steel plates totals 530. Reproducibility was confirmed by repeating each measurement twice. Fig. 5(a) shows the results of the reflection measurements. In the outer side of the torus, the RGB values of almost all of the stainless steel plates are low, which indicates a low reflection coefficient. On the other hand, in the inner side of the torus, the RGB values are high, except for the area near the divertor plates. Fig. 5(b) shows a developed view of the measured stainless steel plates. These results suggest that the outer side of the torus is a deposition dominant area and the inner side of the torus is mainly an erosion dominant area. The reflection coefficient of the stainless steel plates should be determined by the competition between the deposition and erosion processes, which depend on parameters such as the distance to the plasma and the angle of view from the divertor plates. In Ref. [7], it is shown that the RGB value is high when the stainless steel plates are located near the plasma and low when they are located far from the plasma, which suggests a relation between the reflec-

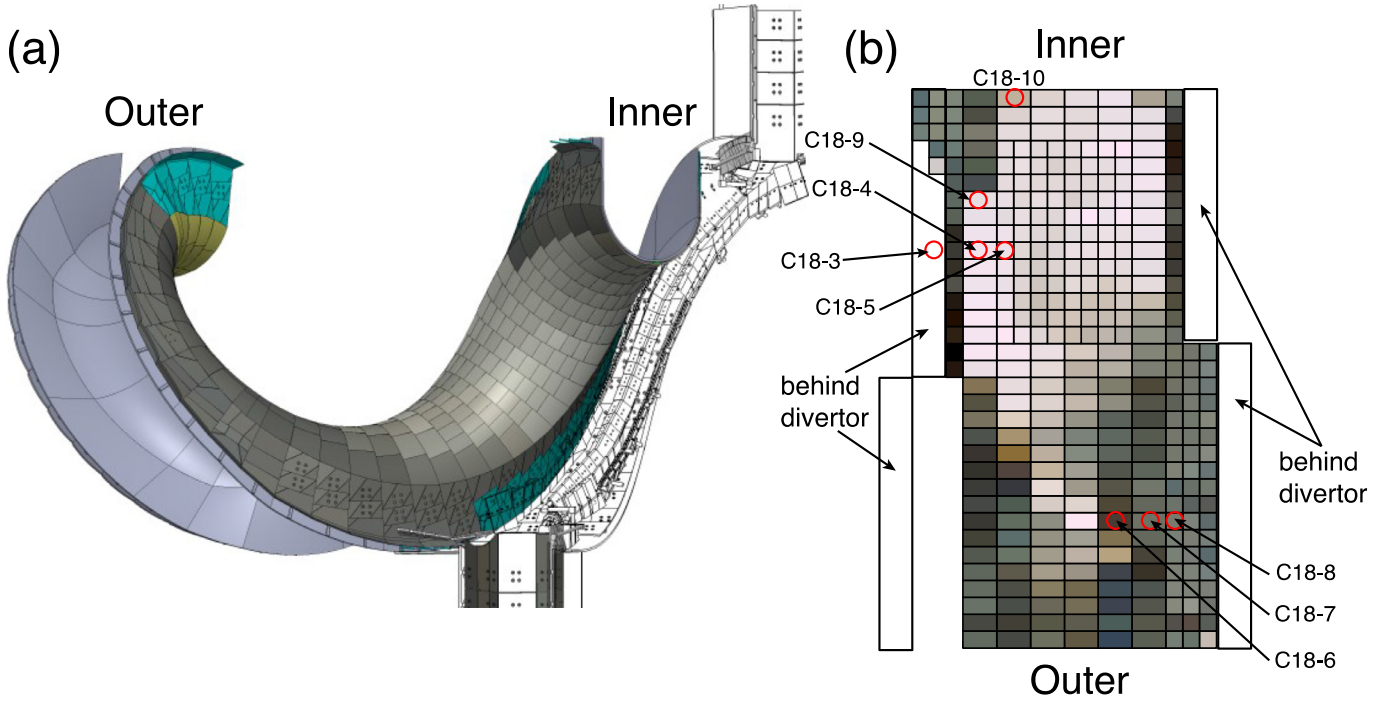

Fig. 5. (a) CAD showing the averaged RGB distribution of the measured stainless steel plates and (b) developed view of the real color distributions. The position of the long-term exposed samples is shown in (b). C18-11 and C18-12 are not shown because these samples are not placed on the coil can. The sample locations are also shown in Fig. 5(b).

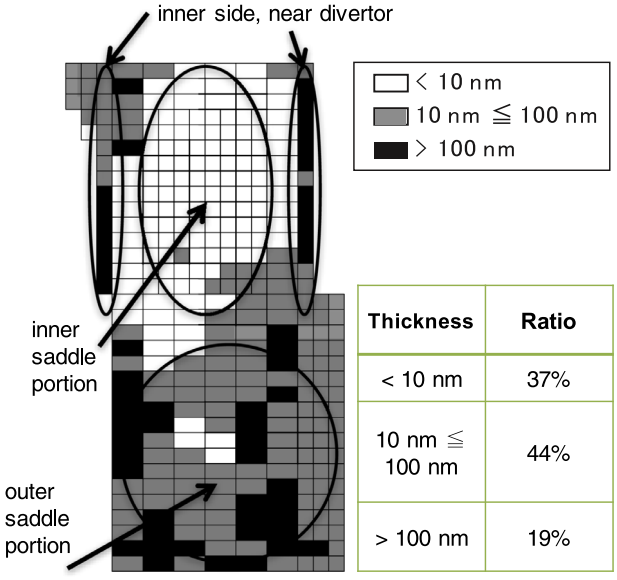

Thickness	Ratio
< 10 nm	37%
10 nm ≦ 100 nm	44%
> 100 nm	19%

Fig. 6. Distribution of the deposition layer thickness. The distribution of thickness is divided into three main parts, the inner saddle portion, the outer saddle portion, and near the divertor on the inner side.

tion coefficient and the distance between the stainless steel plates and the plasma (see the detail in [7]).

3.5. Distribution of the deposition layer thickness

The thickness of the deposition layer was estimated from the distribution of the reflection coefficient on the stainless steel plates by using the single layer model. Fig. 6 shows the distribution of the deposition layer thickness. The outer side of the torus is deposition-dominant, while the inner side of the torus is primarily erosion-dominant, except for the area near the divertor plates. The distribution of the deposition layer on the helically twisted coil revealed that 37% had thickness below 10 nm, 44% had thickness between 10 and 100 nm, and 19% had thickness over 100 nm. These results indicate that approximately 60% of the area on the measured stainless steel plates is coated with a deposition layer over 10 nm, which implies that this area plays a role in the wall retention. If the relation between the deposition layer thickness and the retention amount could be clarified by thermal desorption spectroscopy analysis, then the total retention amount of the deposition layer in the entire first wall could be quantified.

4. Discussion and summary

In the previous section, the thickness of the deposition layer is evaluated using the single layer model. Here, we discuss the sensitivity of the reflection coefficient on the thickness of the deposition layer. The single layer model shows the clear dependence of the reflection on the thickness between 10 nm and 100 nm. However, the dependence of the reflection on the thickness under 10 nm and over 100 nm becomes weak. This is due to the dominant reflection of the mother samples in the case of the thin layer and the dominant reflection of the deposition layer in the case of the thick layer. The averaged RGB of the thickest sample (C18-8) is almost two times the RGB of samples C18-7 and C18-12. The ellipsometric measurements also have the same tendency, implying some physics mechanism. However, the reason remains unclear.

In summary, we employed the wide-range evaluation of the deposition layer thickness distribution on the first wall by optical reflection coefficient measurements using the color analyzer in the following process:

(1) It was confirmed that the averaged RGB value measured by the color analyzer is consistent with the reflection coefficient obtained by the ellipsometric measurement in the long-term exposed samples.
(2) The relationship between the thickness of the deposition layer and the reflection coefficient was revealed by the TEM observation of the long-term exposed samples.
(3) We confirmed that the relationship indicates that the single layer model is valid.

(4) The RGB values were measured for stainless steel plates on the helically twisted coil in one of the 10 toroidal sections of the LHD vacuum vessel and the thickness distribution was evaluated from the RGB values using the single layer model.
(5) The characteristics of the deposition layer thickness distribution were clarified. The outer side of the torus is deposition-dominant, while the inner side of the torus is primarily erosion-dominant, except for the area near the divertor plates. Approximately 60% of the area on the measured stainless steel plates is covered with the deposition layer and may play a role in the wall retention.

In future, if the relation between the deposition layer thickness and the retention amount could be clarified by thermal desorption spectroscopy analysis, then the total retention amount in the deposition layer may be quantified for the entire first wall. Thus, the wide-range evaluation of the thickness distribution of the deposition layer based on the method used in this study is expected to be feasible in other devices, such as ITER, in order to identify the deposition pattern.

Acknowledgments

This work was performed with the support and under the auspices of the Collaboration Research program of the National Institute for Fusion Science (NIFS) (NIFSUMPP003-1) and a Sasakawa Grant for Science Fellows (SGSF) from The Japan Science Society (Grant Number F16-103).

References

[1] H. Kasahara, et al., Proceeding of 25th Fusion Energy Conference (St. Petersburg, 16–20 Sept. 2013) EX/7-3F, 2014.
[2] G. Motojima, et al., J. Nucl. Mater. 463 (2015) 1080.
[3] M. Tokitani, et al., J. Nucl. Mater. 463 (2015) 91.
[4] R. Pugno, et al., J. Nucl. Mater. 390-391 (2009) 68.
[5] P. Wienhold, et al., J. Nucl. Mater. 241-243 (1997) 804.
[6] http://www.atengineer.com/pr/hitachikinzoku/company (in Japanese).
[7] G. Motojima, et al., Plasma Fus. Res. 10 (2015) 1202074.
[8] Karsten Hinriches, et al., in: Ellipsometry of Functional Organic Surfaces and Films, Springer, 2013, p. 16.
[9] K. Ono, et al., J. Nucl. Mater. 463 (2015) 952.